Explainable Machine Learning Algorithm and Hardware for Surgical Robotics

Tian Qijia
Department of Electrical and Electronic Engineering, The University of Hong Kong, u3577272@connect.hku.hk

Abstract - **Deep learning techniques have shown promise in accurate segmentation tasks in medical imaging, particularly in breast cancer diagnosis. This project endeavors to develop an AI-driven segmentation approach tailored for breast tumor delineation, focusing on efficiency and interpretability. The primary objective is to design an Attention UNet model capable of achieving high segmentation accuracy while addressing computational constraints commonly encountered in medical imaging tasks. The methodology involves extensive experimentation, including data preprocessing, model training, and evaluation, culminating in robust segmentation performance metrics. The results reveal the model's high and stable accuracy in segmenting images, though the Intersection over Union in the evaluation metrics indicates some underperformance. This highlights the imperative for continued research aimed at not only improving the model's interpretability but also expanding its utility across a variety of medical imaging modalities. Recommendations encompass acquiring more extensive annotated datasets and delving into sophisticated architectural enhancements to bolster the model's robustness and viability for deployment in real-world scenarios. Additionally, it is advised to swiftly design and implement high-performance, low-power hardware solutions to complement these advancements.**

Index Terms - Attention UNet, Explainable machine learning, Hardware design, Image segmentation

1. INTRODUCTION

Medical image segmentation, especially for breast cancer diagnosis, has greatly benefited from deep learning advancements, notably through the UNet architecture introduced by Ronneberger et al. in 2015. This model, recognized for its adequate structure delineation in medical images via convolutional layers and skip connections, has significantly impacted breast tumor segmentation [1]. Further research, like Singh et al.'s study, confirms UNet's strength in segmentation tasks, showcasing high accuracy, IoU, and sensitivity, thereby affirming its prominence in the domain [2]. UNet's efficiency with limited datasets meets a crucial demand in medical imaging for precise pathological delineation, which is vital for diagnosis and treatment strategies. Despite the rise of Transformer-based models, UNet and its derivatives remain fundamental in medical image segmentation, with ongoing challenges in efficiency and interpretability.

This project aims to develop an AI-driven image segmentation approach to delineate breast tumors while providing interpretable segmentation maps efficiently. This approach aims to reduce the time and effort required for medical professionals to analyze medical images, thereby alleviating their workload and improving diagnostic accuracy.

The importance of this work lies in its potential to alleviate the burden on medical professionals by providing a fast and accurate method for breast tumor segmentation. By automating this process and providing interpretable results, the proposed approach can assist clinicians in making more informed decisions, ultimately improving patient care and outcomes.

This project focuses on segmenting breast tumor regions from 2D ultrasound images, categorizing them into normal and pathological regions. It also considers working with a relatively low quantity of image data and limited computational resources, such as those available in environments like Google Colab.

The primary deliverable of this research is the Attention UNet model, aiming to achieve high segmentation accuracy while providing interpretable segmentation maps through mechanisms such as GradCAM and attention activation. Additionally, this project includes the implementation of evaluation metrics such as Intersection over Union (IoU) and Dice coefficient to measure the model's effectiveness and performance in accurately segmenting medical images.

This report unfolds across eight sections: Section 1 introduces the study's focus and its significance. Section 2 examines the UNet architecture and attention mechanisms. Section 3 outlines the methodology behind

the development and assessment of Attention UNet. Section 4 discusses experimental results, including performance metrics. Section 5 explores the hardware design tailored for the algorithm. Sections 6 and 7 show the model's limitations and future work, respectively. Section 8 concludes with a summary and future research directions.

2. THEORETICAL BACKGROUND

In medical image analysis, the choice of dataset is pivotal for developing robust models capable of accurate segmentation. Alongside dataset considerations, the model's design, evaluation metrics, and model interpretability are crucial aspects that contribute to the overall efficacy and trustworthiness of the segmentation framework.

2.1 Choice of Dataset

The model utilizes the Breast Ultrasound Images Dataset from Kaggle [3]. This dataset contains 780 images of breast ultrasounds from females aged 25 to 75 years. It includes explicit annotations, providing original and annotated versions with ground truth labels for tumor regions. The annotations categorize images into normal, benign, and malignant classes, facilitating supervised learning and model evaluation. The dataset's accessibility under the CC0 license allows unrestricted usage.

2.2 Model Design

The UNet architecture, proposed by Ronneberger et al. [1], is selected as the primary framework for this project. Introduced in 2015, UNet is designed explicitly for biomedical image segmentation tasks, demonstrating remarkable effectiveness even with limited training data.

UNet in Figure I is a convolutional neural network structured with a contracting path followed by an expansive path. The input image undergoes convolutional operations, followed by downsampling to reduce spatial dimensions and increase feature channels. The lowest resolution is reached at the bottleneck, transitioning to upsampling for increased spatial dimensions. Concatenation aids in precise localization, with the final output layer mapping the feature vector to segmentation classes.

To enhance interpretability, an attention layer is introduced before concatenating feature maps in the shortcut connections. This mechanism focuses on specific regions of the image, aiding in understanding the decision-making process. This project integrates the attention mechanism into the UNet model to emphasize regions of interest during feature map concatenation, enhancing interpretability.

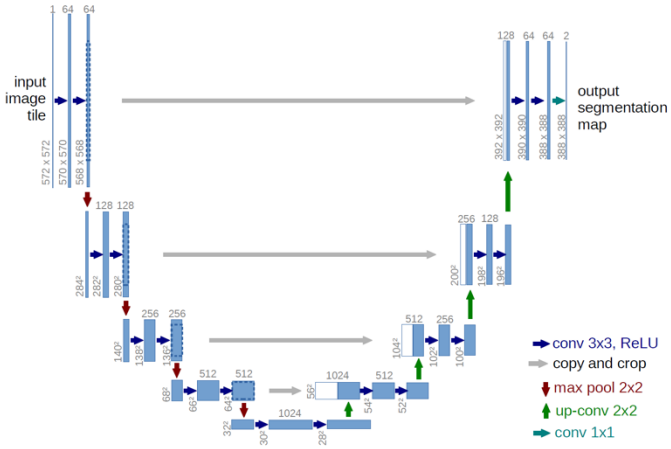

Figure I. UNet Architecture [1]

2.3 Evaluation Metric

Various metrics exist for evaluating image segmentation effectiveness, as outlined by Singh et al. [2]. This paper discusses five key metrics: accuracy, Dice coefficient (Dice), Intersection over Union (IoU), Sensitivity, and Specificity. These metrics are defined based on True Positive (TP), True Negative (TN), False Positive (FP), and False Negative (FN), where A and B represent the ground-truth mask and the model-generated mask, respectively. Among these, IoU and Dice are critical evaluations for assessing segmentation performance. IoU measures segmentation accuracy by calculating the ratio of intersection to union, providing results from 0 to 1, where 1 indicates perfect overlap. The Dice coefficient evaluates accuracy by considering the overlap region's ratio to the average area of the two, balancing true positives and false positives, making it suitable for imbalanced datasets or class segmentation. Additionally, the Dice coefficient is more robust for segmentation with fuzzy boundaries, focusing on region overlap rather than exact pixel matching. These advantages make IoU and Dice essential metrics for evaluating segmentation algorithms' performance and robustness.

$$TP = A \cap B \tag{1}$$

$$FP = \overline{A} \cap B \tag{2}$$

$$FN = A \cap \overline{B} \tag{3}$$

$$TN = \overline{A} \cap \overline{B} \tag{4}$$

$$Accuracy = \frac{TP + TN}{TP + TN + FP + FN} \tag{5}$$

$$Dice = \frac{2TP}{2TP + FP + FN} \tag{6}$$

$$IoU = \frac{TP}{TP + FP + FN} \quad (7)$$

2.4 Model Interpretability

In the realm of artificial intelligence, a delicate balance exists between interpretability and complexity. While sophisticated models such as DNNs excel in tasks like image segmentation, their internal decision-making processes pose a formidable challenge to interpretation. This struggle to balance accuracy and interpretability is a significant hurdle in Explainable Image Segmentation.

Interpretability methods, encompassing visualization-based, surrogate, and intrinsic approaches, are pivotal in shedding light on model decision-making [4]. These methods enhance audience trust in the models and facilitate their validation and improvement, instilling confidence in their reliability.

To better explain, this project adopts various interpretability methods:

- Saliency Map and its variants use gradient information to identify regions of interest, aiding in understanding model decisions.
- GradCAM enhances interpretability by visualizing regions of focus indicated by the Attention layer.
- Occlusion Sensitivity evaluates regions critical to model predictions by occluding different areas.
- The Attention UNet model's attention mechanism improves interpretability by highlighting essential image regions.
- While LIME is not used because the model covers all subclasses, combining interpretability techniques enhances understanding of the model's decision-making process.

In summary, combining interpretability techniques enhances the model's interpretability, credibility, and reliability.

3. EXPERIMENTAL PROCEDURE

The procedure adopts a modular design approach, comprising the design and implementation of components such as the Encoder Block, Decoder Block, Attention Gate, and callback modules. This is followed by model training and result presentation, with each process detailed in subsequent sections.

3.1 Environment Setup

The setup process for model interpretation and visualization in TensorFlow involves installing the `tf_explain` library and importing essential libraries like NumPy, OpenCV, and TensorFlow. These libraries enable the interpretation of model decisions and visualization of internal workings and facilitate data manipulation, model training, and performance evaluation. Specific functionalities for Grad-CAM visualization are also imported from the `tf_explain` library, providing insights into the model's decision-making process and identifying features it relies on for classification or segmentation tasks. Overall, the setup ensures comprehensive analysis and understanding of model behavior.

3.2 Data Input

This segment describes the process of loading and preprocessing images for a dataset. The `load_image` function reads an image from a specified file path using Keras and converts it into a NumPy array. Pixel values are normalized from 0 to 1 and resized to a specific dimension for consistency. Pixel value precision is rounded for computational efficiency. The `load_images` function applies these preprocessing steps to each image path, retaining only the first channel for masks. Processed images and masks are aggregated into arrays for seamless integration into the training and evaluation pipeline. This segment efficiently prepares image data for robust and accurate model development in machine learning applications.

3.3 Encoder Block

The Encoder Block is a fundamental component of a neural network's encoder. It processes input data, extracts features, and reduces spatial dimensions through convolutional layers augmented with dropout regularization. An optional max-pooling layer further reduces spatial dimensions. During the forward pass, the call method applies defined layers sequentially. Depending on the pooling parameter, it returns the output, output, and input data before pooling. The `get_config` method allows retrieval of configuration parameters, enhancing reproducibility and facilitating model serialization. The Encoder Block contributes to feature extraction and dimensionality reduction, improving the model's efficacy and performance.

3.4 Decoder Block

The Decoder Block is crucial for reconstructing spatial information lost during encoding. It handles upsampling and concatenating feature maps from encoder blocks, recovering spatial details for accurate segmentation or reconstruction. The block comprises an upsampling layer to increase spatial dimensions and an `EncoderBlock` instance for further feature processing. During the forward pass, the call method takes input feature maps (X) and corresponding skipped inputs (skip_X), performs upsampling, concatenates feature maps, and passes them through the `EncoderBlock`

instance for final output. The `get_config` method returns configuration parameters like filter number and dropout rate. Overall, the Decoder Block contributes significantly to the model's effectiveness and performance in segmentation and image reconstruction tasks.

3.5 Attention Gate

The `AttentionGate` class is pivotal in the U-Net model, implementing an attention mechanism to focus on relevant spatial regions selectively. It comprises convolutional layers for feature processing, element-wise addition for combining inputs, and attention weight learning to determine region importance. Optionally, batch normalization stabilizes training. The `get_config` method returns configuration parameters like filter number and batch normalization usage. The `AttentionGate` enhances the U-Net architecture by selectively focusing on relevant regions, improving segmentation accuracy.

3.6 Custom Callback

The Custom Callback module offers functionalities for model interpretation and training progress visualization. It includes the compute_guided_backpropagation function for calculating gradients using guided backpropagation, aiding in model interpretation. Additionally, the `ShowProgress` callback class visualizes training progress:

- Visualizing Attention Gate GradCAM Results: Utilizes GradCAM to highlight crucial regions for predictions, enhancing interpretability.
- Visualizing Saliency Maps and Guided Backpropagation: Highlights relevant regions for prediction using saliency maps and guided backpropagation, aiding in model understanding.

These visualizations assist in model debugging, validation, and improvement, with regular updates provided throughout the training process by the on_epoch_end method.

3.7 Main Body

The custom U-Net architecture in Figure II with attention gates for image segmentation consists of interconnected components:

- Encoder Blocks: Four `EncoderBlocks` downsample the input image and extract hierarchical features, generating pooled features and corresponding feature maps before pooling.
- Encoding: An additional encoding block captures high-level semantic information from the input image.
- Attention Mechanism: Four `AttentionGates` emphasize informative regions and suppress irrelevant features selectively.
- Decoder Blocks: Four `DecoderBlocks` upsample features and reconstruct the segmentation mask, incorporating skip connections and attention gates.
- Output Layer: A convolutional layer with sigmoid activation yields the segmentation mask.
- Model Compilation and Training: The model is compiled with binary cross-entropy loss and the Adam optimizer, with custom metrics such as accuracy, IoU, and Dice coefficient. Training parameters include batch size, epochs, and validation split, which are monitored using callbacks.

This architecture enables effective segmentation of input images into distinct regions of interest, which is suitable for various medical image analysis tasks.

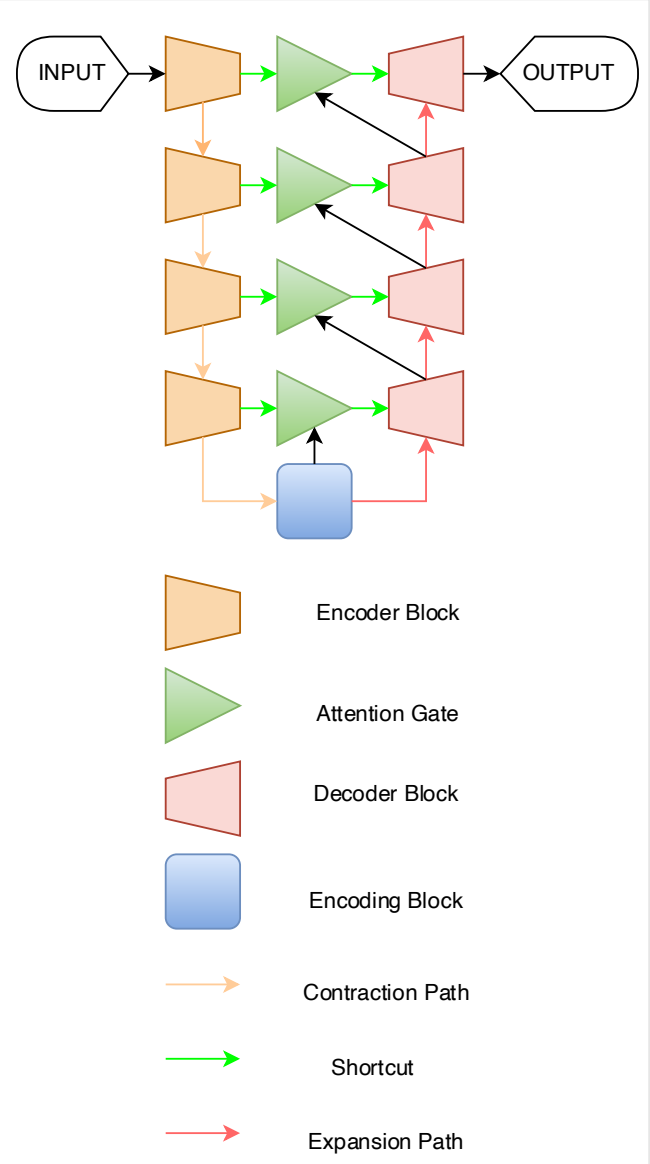

Figure II. Attention UNet Stucture

3.8 Evaluation

The evaluation section includes visualizing the trained model's performance metrics and utilizing occlusion sensitivity mapping for interpretation:

- Model Performance Visualization: Subplots show training and validation metrics (loss, accuracy, IoU, Dice coefficient) across epochs, accessed from the `results.history` dictionary.
- Segmentation Results and Confidence Maps: Visualizations display original images, ground truth masks, predicted masks, processed masks (thresholded predicted masks), and confidence maps of predicted masks for a random subset of images. The processed mask is generated using a confidence threshold of 0.5.
- Occlusion Sensitivity Mapping: A subplot visualizes the occlusion sensitivity map, revealing the model's sensitivity to specific image regions. Windows are iteratively slid across each image, comparing predictions between original and occluded images to compute sensitivity maps. Aggregating sensitivity maps produce the final map, highlighting regions crucial for segmentation.
- Saliency Maps and Guided Backpropagation: Saliency maps and guided backpropagation techniques highlight the most relevant regions of the input image for prediction. Saliency maps indicate regions of high importance, while guided backpropagation emphasizes these regions by illustrating gradients of the output with respect to the input image. These visualizations offer insights into the model's decision-making process and contribute to model understanding and validation.

These visualizations aid in evaluating model performance, understanding segmentation decisions, and identifying significant image regions influencing predictions. Occlusion sensitivity mapping enhances model interpretability by revealing attention and feature importance.

4. RESULTS & ANALYSES

This section presents a comprehensive overview of the U-Net model's performance and various visualization techniques employed for image segmentation.

4.1 Masks and Maps

Figure III showcases various image segmentation results from extensive training, including the ground truth original mask and its closely matching predicted counterpart, with minor differences noted on the left. A processed mask further refines segmentation by eliminating low-confidence areas, while a confidence map displays bright regions of high certainty in predictions. The occlusion sensitivity map accentuates crucial boundary areas around the tumor. These results underscore the model's compelling performance in accurately delineating boundaries and reducing false positives and negatives through post-processing. Bright spots in the confidence map reflect well-converged training, and the occlusion map's focus on critical edges points to successful feature learning for segmentation.

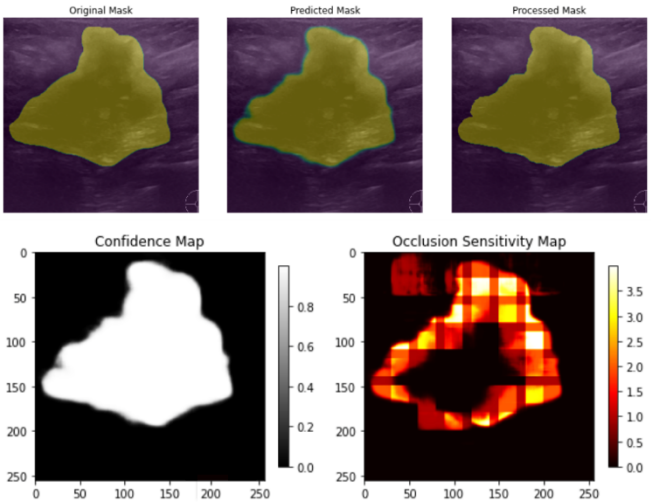

Figure III. Masks and Maps

Figure IV illustrates an alternative approach for explaining ultrasound image segmentation through a Saliency Map that accentuates influential image regions, especially around tumor edges, and Guided Backpropagation, which pinpoints key features for model predictions by adjusting ReLU function gradients, resulting in a visualization that, while similar to the saliency map, appears sparser.

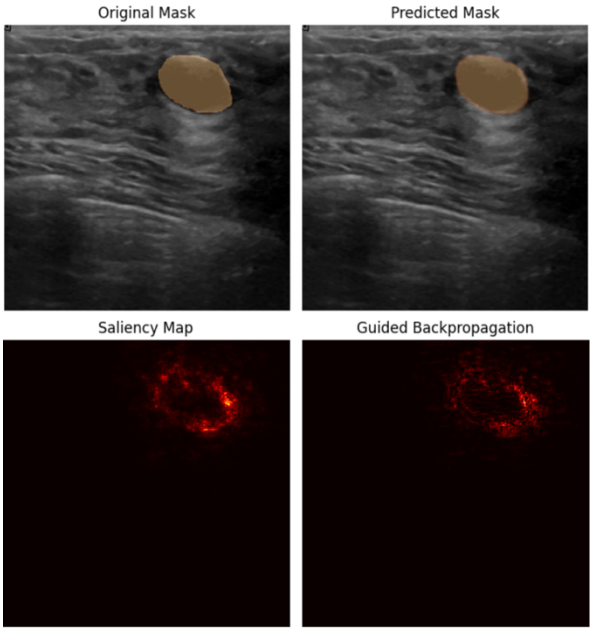

Figure IV. Saliency Map & Guided Backpropagation

The concordance between the original and predicted masks corroborates the segmentation's precision. The saliency map and guided backpropagation underscore critical areas, bolstering the identification of diagnostic features and reinforcing the model's capability to accurately capture essential segmentation details.

4.2 Model Performance Metrics

Figure V reveals significant insights into the model's performance across key metrics over epochs, focusing on loss, accuracy, and IoU, which collectively illustrate the model's learning efficacy and precision in segmentation tasks. The model demonstrates a steady decrease in both training and validation loss, indicative of effective learning, with training loss diminishing to around 0.01 and validation loss stabilizing near 0.1. This pattern of minimal fluctuations suggests a robust training process with limited overfitting, underscored by the convergence of training and validation losses.

Accuracy metrics exhibit an overall positive trajectory despite some variability, highlighting an improvement in the model's generalization ability. Validation accuracy consistently hovers around 0.98, reflecting the model's high predictive accuracy in unseen data. IoU scores also follow an upward trend with fluctuations, indicating gradual enhancements in the model's segmentation accuracy. Training IoU peaks at approximately 0.7, while validation IoU attains around 0.61, maintaining a narrow gap between training and validation performance.

These fluctuations in performance metrics might stem from factors like learning rate adjustments via the Adam optimizer or inherent data variability. Nonetheless, the similarity observed between training and validation metrics suggests a well-generalized model potentially influenced by a carefully curated validation set or the application of effective regularization techniques.

Comparing these outcomes to benchmarks, such as the UNet model's IoU scores ranging between 0.66 to 0.77 in breast tumor segmentation, as reported by V. K. Singh et al. [2], illustrates that our model's performance is not only competitive but also indicative of its capability to achieve state-of-the-art results. This benchmark comparison validates the model's effectiveness and underscores its potential for precision in medical image segmentation tasks.

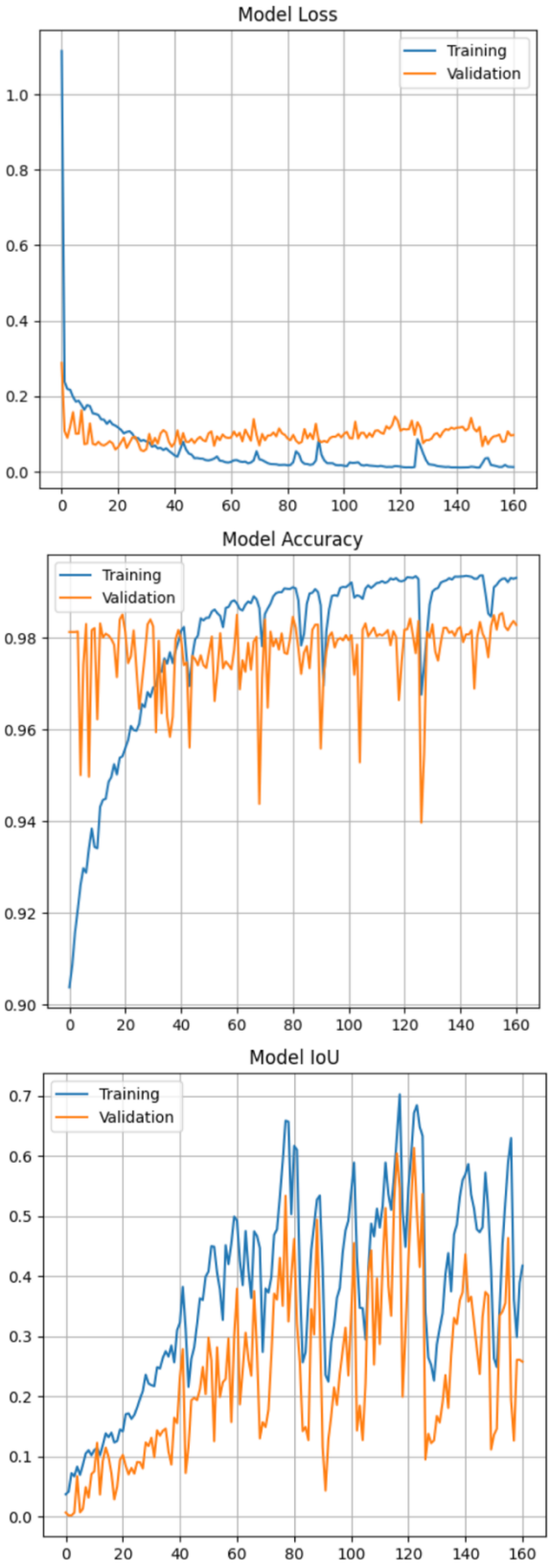

Figure V. Model Performance Metrics

5. HARDWARE DESIGN

Incorporating the Attention UNet image segmentation technology into the medical sector necessitates hardware that is energy-efficient yet powerful to ensure seamless integration with medical devices.

The hardware architecture, illustrated in Figure VI, is designed with a dual-memory system comprising off-chip and on-chip memory to optimize data management and processing speed. Off-chip memory handles large-scale storage needs, including segmented images and raw images or video data, in addition to storing the model's extensive parameters. On-chip memory, known for its smaller size but faster access, facilitates swift data processing and interaction with computational units and the Attention Monitor, which provides immediate feedback on the model's focal areas. This setup allows for quick adjustments to the system's monitoring and control, enhancing the model's responsiveness. Additionally, by storing immediate inputs and feature maps, the on-chip memory supports efficient data flow, reducing the frequency of accessing off-chip memory and thereby streamlining overall computation.

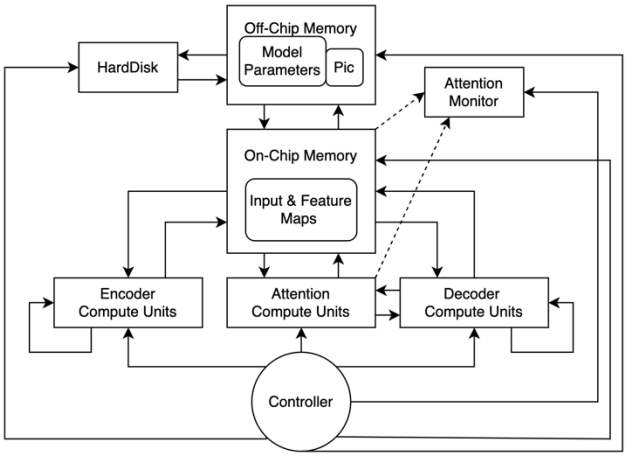

Figure VI. Hardware Structure

The computational process is segmented into three specialized units—Encoder, Attention, and Decoder—each designed for distinct phases of the task. The Encoder pulls input from on-chip memory, executing iterative calculations to extract features, which are then refined by the Attention unit. This refinement prioritizes crucial image areas, enhancing the model's focus. The Decoder, receiving focused features from the Attention unit, reconstructs the segmented image. This streamlined workflow minimizes memory access, improving efficiency and performance during both training and inference phases. All hardware elements are orchestrated by a central controller that maintains the operational harmony of the system.

Performance evaluation includes:

- Execution Time: Essential for real-time applications, reflecting computational speed and efficiency.
- Memory Usage: Indicates the system's capacity for efficient data handling, crucial for maintaining performance without frequent data transfers.
- Instructions Per Cycle (IPC) and Cycles Per Instruction (CPI): These metrics provide insights into the computational efficiency and resource utilization of the hardware, guiding optimizations for enhanced performance.

These benchmarks are selected to directly assess the system's ability to meet the stringent requirements of medical imaging tasks, focusing on speed, efficiency, and accuracy.

For model debugging and validation, datasets from within the algorithm are used as inputs fed into the off-chip memory. Post-simulation validation, real-world trials with camera image data streams can be compared against the simulation results to ensure reliability and efficiency.

6. LIMITATIONS

Despite the Attention UNet model showing promise in breast cancer image segmentation, it encounters significant limitations that impede its practical application in the medical field. These challenges span from dataset constraints to issues with training stability, an overly ideal model environment, reliance on supervised learning, interpretability concerns, and conceptual gaps in hardware design.

Firstly, the dataset's limited scope of merely 780 images starkly contrasts with the expansive variety needed for a real-world application. This limitation hampers the model's ability to adapt and accurately segment images with irregular tumor shapes. A more substantial and diverse dataset could enhance the model's generalization capabilities.

Moreover, the model's training process is marred by instability, exhibiting severe fluctuations in key performance indicators like IoU coefficients. Such unpredictability is not conducive to the precision and reliability required in medical diagnostics. This inconsistency suggests a discrepancy between laboratory conditions and the stringent demands of clinical environments.

The model's approach, focusing on binary image segmentation, overly simplifies the nuanced reality of medical imaging. Real-world scenarios often necessitate multi-class segmentation to distinguish between various types of tissues and pathological states accurately.

Advancing the model's learning to encompass a broader range of features through training could significantly improve segmentation accuracy.

Another critical challenge lies in the model's dependency on supervised learning, which requires accurately annotated datasets. This dependency is particularly problematic for complex images where accurate annotation by medical professionals is challenging, thereby limiting the model's training in such cases.

Interpretability technologies employed within the project, although helpful, fall short of integrating with medical theoretical knowledge. This gap undermines the scientific rigor and credibility of the model's segmentation basis, making it difficult to trust the model's decisions without a solid theoretical grounding.

Finally, transitioning from the model's computational parameters to a tangible hardware design remains conceptual. Detailing the engineering aspects necessary for converting computational functions into effective hardware operations is essential for the model's deployment in real-world settings.

7. Future Work

In light of the limitations outlined, several avenues exist for improvement in the Attention UNet model's application to breast cancer image segmentation. These enhancements aim to address the current model's shortcomings and expand its capabilities, ensuring it can meet the rigorous demands of medical diagnostics more effectively.

Acquiring a broader and more diverse dataset of ultrasound images of breast cancer is imperative. This expansion could involve collecting images without restrictions to increase diversity and introducing noise to improve the model's generalization capability and prevent overfitting. Additionally, accommodating unlabeled or semi-labeled samples could alleviate the preparatory burden, making the model more versatile and less dependent on extensively annotated datasets.

Improving the evaluation metrics is another critical area of future work. By filtering out both inferior and excellent outliers before averaging, metrics like IoU and Dice can be stabilized, ensuring they more accurately represent the model's performance. Implementing a monitoring mechanism to oversee the training process, which could interrupt training upon detecting a lack of improvement over several epochs, could optimize training efficiency and outcomes.

Enhancing the hardware setup to surpass the efficiency of general-purpose computers significantly is essential. This entails not only refining the hardware architecture but also conducting extensive testing to guarantee the system's capability to support the computational demands of sophisticated deep-learning models. Achieving this would improve the model's practical applicability and performance in real-world settings.

Integrating the model's training, inference, and interpretation results with a large language model could offer more coherent and accessible explanations for its decisions. This would not only improve the model's usability for medical professionals but also increase trust in its predictions.

Lastly, leveraging recent advancements in the field, such as incorporating a Transformer architecture into the Attention UNet model, holds promise for significantly enhancing predictive performance. As exemplified by the UNet Transformer architecture, introducing a Transformer could lead to more accurate segmentation of irregularly shaped organs and tissues in medical imaging tasks. This approach could address the current model's limitations in handling complex segmentation scenarios.

8. Conclusion

This project focused on developing the Attention UNet model for medical image segmentation, targeting breast cancer detection in ultrasound chest images. Integrating artificial intelligence into medical image analysis can alleviate healthcare professionals' burden, potentially reducing misdiagnosis and missed diagnoses. The model's interpretability enhances medical personnel's understanding of segmentation, increasing acceptance of new technologies. Additionally, the Attention UNet operates efficiently with limited data and computational resources thanks to its modular design of Encoder Blocks, Decoder Blocks, and Attention Gates.

The Attention UNet model performed well overall, with decreasing loss and high accuracies during training. While IoU fluctuated, they showed an increasing trend, indicating improved segmentation performance. Despite challenges like irregular tumor shapes, the model demonstrated precise segmentation results with minimal overfitting tendencies.

Practically, the model automates medical image preprocessing, reducing physicians' workload and addressing healthcare resource constraints. However, further research is needed to enhance interpretability and extend the model's applicability to diverse medical image modalities. Despite achievements, limitations like fluctuating metrics and dataset size constraints were encountered, along with challenges integrating local interpretability techniques like LIME due to mask size

mismatches. Moving from theory to practice also requires careful hardware design and simulation of hardware components to ensure the model works effectively in real-world conditions.

Future research will focus on acquiring larger, precisely annotated datasets, improving evaluation metrics, and exploring advanced architectures like Transformer UNet for multi-class segmentation. Iterative improvements in interpretability techniques akin to large language models could revolutionize medical image analysis. In culmination, the development and rigorous testing of hardware specifically designed to optimize the performance of the Attention-UNet algorithm will be pivotal, ensuring that these technological advancements are fully realized and effectively implemented in clinical settings.

ACKNOWLEDGMENTS

I extend my sincere appreciation to Dr. Can Li for their exceptional guidance, support, and mentorship throughout this project. His profound expertise, unwavering encouragement, and invaluable feedback have been pivotal in shaping the trajectory of my research and fostering my academic development.

Furthermore, I express my gratitude to Dr. Can Li's esteemed doctoral student, Bo Wen, for his valuable assistance, insightful contributions, and collaborative spirit. Their dedication and expertise have significantly enriched my understanding of the subject matter and enhanced the quality of my work.

REFERENCES

[1] O. Ronneberger, P. Fischer, and T. Brox, "U-Net: Convolutional Networks for Biomedical Image Segmentation," arXiv.org, https://arxiv.org/abs/1505.04597 (accessed Mar. 7, 2024).

[2] V. K. Singh et al., "Breast tumor segmentation in ultrasound images using contextual-information-aware deep adversarial learning framework," Expert Systems with Applications, vol. 162, p. 113870, Dec. 2020. doi:10.1016/j.eswa.2020.113870

[3] W. Al-Dhabyani, M. Gomaa, H. Khaled, and A. Fahmy, "Dataset of breast ultrasound images," Data in Brief, vol. 28, p. 104863, Feb. 2020. doi:10.1016/j.dib.2019.104863

[4] Q. Teng, Z. Liu, Y. Song, K. Han, and Y. Lu, "A survey on the interpretability of deep learning in medical diagnosis," Multimedia Systems, vol. 28, no. 6, pp. 2335–2355, Jun. 2022. doi:10.1007/s00530-022-00960-4

AUTHOR INFORMATION

Tian Qijia, Computer Engineering Student, Department of Electrical and Electronic Engineering.